THE JOURNAL OF PHYSICAL CHEMISTRY B

ARTICLE

pubs.acs.org/JPCB

Broadband Electric Spectroscopy at High CO_2 Pressure: Dipole Moment of CO_2 and Relaxation Phenomena of the CO_2−Poly(vinyl chloride) System

Vito Di Noto,*[,†] Keti Vezzù,[‡] Fosca Conti,[†] Guinevere A. Giffin,[†] Sandra Lavina,[†] and Alberto Bertucco[‡]

[†]Department of Chemical Sciences, University of Padua, Via F. Marzolo 1, I-35131 Padova, Italy
[‡]Department of Chemical Engineering, Principles and Practice (DIPIC), University of Padua, Via F. Marzolo 9, I-35131 Padova, Italy

ABSTRACT: Broadband electric spectroscopy (BES) is a technique that shows promise in studying the interactions of dense or supercritical gases with polymers, particularly with respect to chain mobility. Polymers that are treated with dense gases show a reduction in the viscosity, glass transition, and melting temperature. A high pressure cell for BES has been constructed that can be used from ambient temperature and pressure to 353 K and 15 MPa and over a frequency range from 20 Hz to 1 MHz. In the past, the dielectric constant of CO_2 was determined by measurements at only one or two frequency values. New instrumentation and technology allow this experiment to be expanded to cover a wider frequency range. BES measurements of CO_2 do not show any relaxation peaks in the permittivity from 20 Hz to 1 MHz and 1 to 6 MPa. By these measurements, the CO_2 dielectric constant was evaluated between 0.1 and 6 MPa. Cell testing with poly(vinyl chloride) (PVC) at 323 K and CO_2 pressures from 0.1 to 13 MPa indicate an increase in the chain segmental motion at high pressures resulting from a reduction in the glass transition temperature of the PVC−CO_2 system due to plasticization by CO_2.

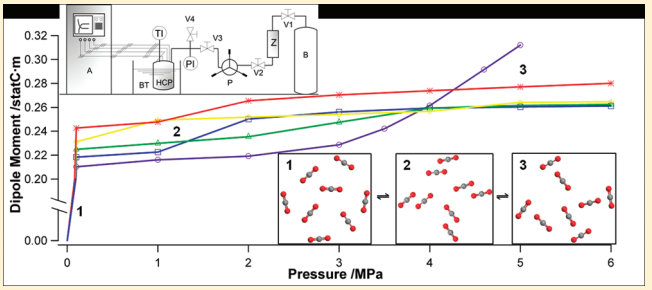

INTRODUCTION

Recently there has been significant interest in using supercritical fluids (SCFs) in the development of polymer technologies. Many compressed gases are soluble in amorphous polymers at relatively low pressures, which can result in swelling and plasticization.[1] In particular, carbon dioxide (CO_2) has been studied because it has a critical point close to ambient conditions (T_c = 304.25 K, P_c = 7.4 MPa).[2] CO_2 gas is quite soluble in polymers at relatively high pressure and causes considerable plasticization effects, matrix swelling, lowering of both the glass transition temperature (T_g) and melting point (T_m).[3] As a result, SCFs have received attention for modification of the physical−chemical properties of polymers through solvent-free, low-polluting methods of polymer processing.[4−7] SCFs have liquid-like densities and gas-like low viscosities that lead to high rates of molecular diffusion, often resulting in superior mass-transfer rates as compared to that of liquids.

In the presence of CO_2, some polymers exhibit an improvement in chain mobility and an increase in salt dissociation, resulting in an improvement in the conduction.[3] Often the properties of the material are permanently changed even after the SCFs have been removed.[4,6−8] The CO_2 molecules in these systems likely act as a plasticizer through Lewis acid−base interactions with electron-donor species, such as carbonyl groups.[3] This plasticization effect can significantly influence the electric properties of the polymer.[6,7]

The chain mobility of macromolecules can be studied with electric spectroscopy.[8] In electric spectroscopy, the sample is subjected to an alternate current at a fixed or variable frequencies and then the electric response of the material analyzed. The use of variable frequencies allows the study of the molecular dynamics of the material. For example, electric measurements under CO_2 pressure have been used to evaluate the solubility of the polymer in supercritical CO_2.[9,10] It is essential to examine the interaction between CO_2 and polymers at different pressures and temperatures. In this work, a high pressure cell for electric measurements, along with the accompanying experimental apparatus, is described.

Recently, some groups have built electric cells to study the electrical properties of polymers under CO_2 pressure or mixtures in supercritical phases.[11−15] These works showed the effect of the CO_2 plasticization on the relaxation process of the polymer.[13,15] Previously, the electric dipoles of CO_2 have been determined by different methods such as the heterodyne null method or viscosity measurements.[16−18]

This work has three aims. The first is to build a system without electrical dispersion and gas leakage, which has the capability to measure the electrical spectra of materials at low permittivity under CO_2 pressure. The second aim is to study intermolecular interactions in supercritical CO_2, focusing on the interaction between CO_2 molecules and CO_2 aggregates as a function of temperature and pressure. Finally, the third aim is to study the interaction

Received: May 10, 2011
Revised: June 15, 2011
Published: June 16, 2011

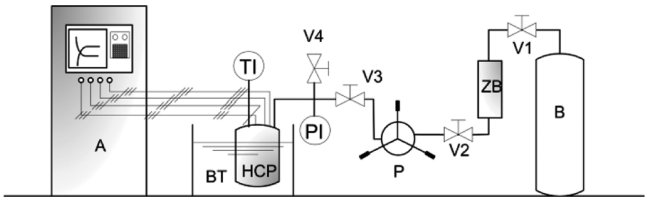

Figure 1. Schematic of the experimental setup for high pressure dielectric measurements: HCP, high CO_2 pressure cell; P, manual pump; ZB, zeolite bed; BT, thermostatic bath; B, CO_2 gas cylinder; V, on−off valves, PI, pressure indicator; TI, temperature indicator; A, impedance analyzer.

between CO_2 and supramolecular molecules. A preliminary study of poly(vinyl chloride) with CO_2 is presented here. Poly(vinyl chloride) is chosen because it is one of the most studied and straightforward systems for dielectric spectroscopy.[19]

MATERIALS AND METHODS

Materials. Carbon dioxide (CO_2) (purity 99.995%) was purchased from Sapio. Poly(vinyl chloride) (PVC, molecular weight = 90 000 Da, glass transition temperature = 348.15 K) and tetrahydrofuran (THF, purity ≥99.9%) were purchased from Sigma-Aldrich. A 100 μm PVC film was obtained by solvent casting from 2.5% (w/w) PVC/THF solution onto a Teflon plate. The solvent was evaporated at room temperature overnight. The surface of the films was sputtered with gold using ion sputtering methods (Edwards S 150 A). A commercial resistor (1.0 MΩ) and capacitor (47 pF) were used to calibrate the cell. Glass fibers with diameter of 120 μm, which were used as a separator between the electrodes, were obtained by removing the covering from an optical transmission data cable.

Electric Measurements under Gas Pressure. The experimental setup for the electric measurements at controlled gas pressures is shown in Figure 1. At the core of the setup is a high CO_2 pressure cell (HCP), which can be filled with CO_2 gas present in gas cylinder B. The gas is predried over a type-A zeolyte bed (ZB) made accessible by opening valves V1 and V2. A manual screw pump (P, SITEC (PTC, Genova, Italy)) allows the cell pressure to be increased to pressures higher than the gas cylinder (B, 6 MPa). The pump is cooled by a thermostatic bath to maintain the CO_2 in a subcooled condition (ca. 278 K). The temperature of the HCP is controlled by a second thermostatic bath (BT) in the range from 283 to 350 K within ±0.05 K and is monitored by a resistance sensor (TI, PT 100 Ω (RCS, Padova, Italy)). The pressure of the HCP is monitored by a Bourdon gauge (PI, error = ±0.02 MPa). The experimental electric spectra are recorded in the frequency range from 20 Hz to 1 MHz by an Agilent 4284A Precision Impedance Analyzer (A).

High CO_2 Pressure Cell (HCP) for Electric Measurements. The HCP cell, illustrated in Figure 2, consists of two electrodes and a support system. The latter is developed to avoid electric dispersion and to reduce the possibility of modulation of the film thickness. Higher compression of the film would result in variation of the film thickness as the temperature is increased, while lower compression could lead to variation caused by swelling of the polymer matrix due to CO_2 solubilization. The measurement electrodes are two stainless steel discs polished to mirror quality. Electric insulation of the electrodes from the outer body of the cell was guaranteed by Teflon and quartz cylindrical spacers as in Figure 3.

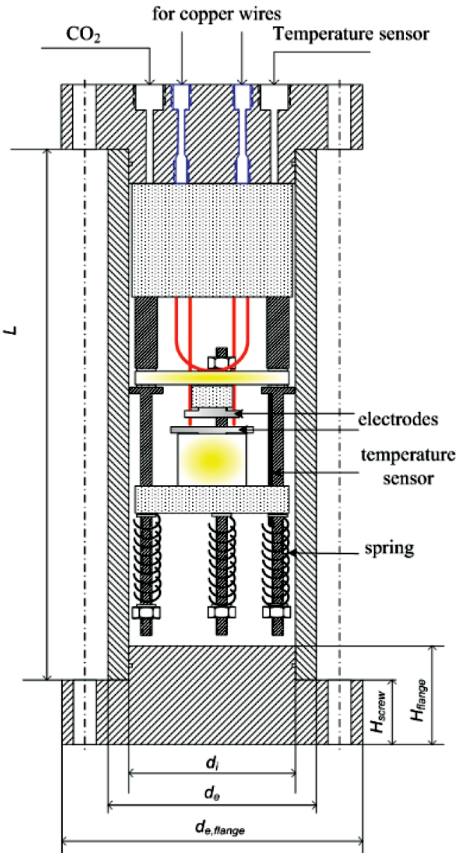

Figure 2. High pressure cell for dielectric measurements in the presence of dense CO_2.

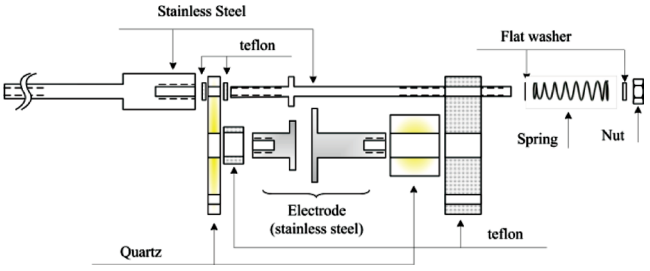

Figure 3. Setup of the measurement electrodes.

The electrode assembly is protected by a stainless steel cylindrical cell bolted together with two flanges and sealed with neoprene O-ring. The top flange has holes for the bolts, gas inlet/outlet, temperature sensor, and electric contacts (Figure 2). Stainless steel 1/8 in. NPT connections are used for the temperature sensor and the CO_2 feed pipe. The copper wires are inserted into 1/16 in. PEEK tubing and are sealed with a stainless steel compression Valco ferrule. The wires are welded to an electric cable suitable for high frequencies located on the top of the flange. The outer body of the cell is grounded together with the thermostatic bath and the rest of the system.

The geometric parameters of the HCP are summarized in Table 1 and determined as described in Appendix A.

Electric Circuit To Test the HCP. The HCP performance was tested by a parallel circuit based on a 47 pF capacitor and a 1.0 MΩ resistor ($RC_{||}$ circuit). In Figure 4 the scheme of the $RC_{||}$

dx.doi.org/10.1021/jp2043448 |J. Phys. Chem. B 2011, 115, 9014–9021

Table 1. Geometric Dimensions of the High Pressure Cell for Dielectric Measurements under Gas Pressure

element	dimension (mm)
external diameter of cell, d_e	73
internal diameter of cell, d_i	64
length of cell, L	230
external diameter of flanges, $d_{e,flange}$	125
height of flanges, H_{flange}	43
number of screw bolt, n_{bolt}	4
height of screw, H_{screw}	28

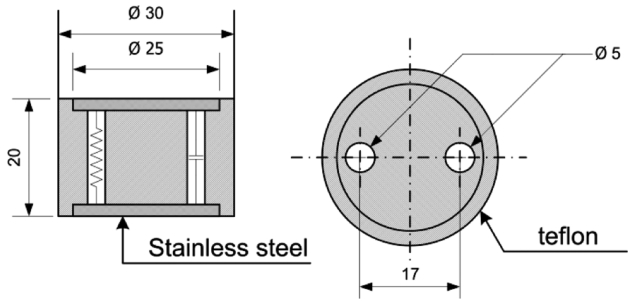

Figure 4. Schematic of RC$_{||}$ test circuit employed to study the electric response of the high pressure cell. Ø = diameter in mm.

circuit is reported. The resistor and the capacitor are separated with a Teflon spacer, while electric contact with the cell electrodes is obtained by two stainless steel discs.

Sample Assembly for the Electric Measurements. In order to measure the gas permittivity, three glass fibers with a thickness of 120 μm are placed between the two stainless steel electrodes of the HCP as in Figure 5a. Three compression springs ensured a constant spacing (120 μm) between the electrodes during the permittivity measurements of CO_2. The polymer film, sputtered with gold on both sides, is sandwiched between the HCP electrodes as in Figure 5b. The electrodes are carefully placed and kept in position by three compressing springs as in Figures 2 and 3.

RESULTS AND DISCUSSION

BES measurements are based on the electrical response of the sample to an alternate current stimulus. It is very important to reduce or avoid external dump tension, eddy capacitance, and inductance, which could occur due to contact points of different materials and to the welds. In addition, perfect electrical connections are necessary in all structural parts of the cell to ensure a good Faraday cage. To achieve accurate and reproducible measurements, the contact surface between the measuring electrode and the sample must be considered. Roughness of the electrode metal and the film at microscopic level can change the contact surface, so the electrodes are polished to mirror quality and the film surfaces are sputtered with gold. The electric response or insulation of HCP is determined using a known RC$_{||}$ circuit as described in the Materials and Methods.

Electric Test of the HCP Cell. The HCP performance was tested using the RC$_{||}$ electric circuit embedded in a Teflon insulating core, as shown in Figure 4. Two different connections were used: (1) the RC$_{||}$ test circuit directly connected to the HP 4284A precision analyzer; and (2) the RC$_{||}$ test circuit within the

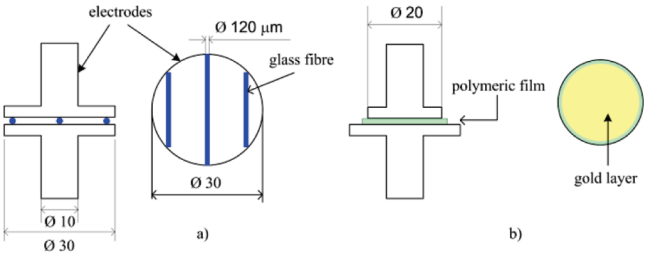

Figure 5. Schematic of sample preparation for dielectric measurement: setup for gas measurement (a), and for film measurement (b). Ø = diameter in mm.

sample compartment of the HCP. It should be noted that the resistor and the capacitor in the RC$_{||}$ test circuit are well separated to avoid any inductive effects that could occur between the two electric elements. Figure 6a shows the impedance of the test circuit recorded at ambient pressure for both connections. The real component of the impedance, Z', is reported on the left axis, while the imaginary component, Z'', is on the right axis. It is noteworthy that the patterns of the RC$_{||}$ test circuit's electric response are the same in both configurations. To exclude the possibility of current dispersion in the HCP cell due to the plasticization of insulating material by CO_2, the experiment is conducted both in the presence and in the absence of CO_2. From the representation of $-Z'$ versus Z'', it is possible to observe that the semicircle is preserved and the gas does not appear to have an effect on the electrical junctions, i.e., soldered joints and insulation materials (data not shown).

The value of the resistance (R) was determined from the representation of Z'' versus Z' by the method of equivalent circuits as described elsewhere,[20] while the capacitance (C) was determined from the frequency of the maximum of the Z'' peak position, f_{peak}, considering that $RC = 1/(2\pi f_{peak})$. The estimated values of R and C are 1.0019 MΩ and 48.06 pF for configuration 1 and 1.0022 MΩ and 47.05 pF for configuration 2. These results are comparable to those of the nominal values of the commercial electrical elements used to build the test circuit, which are reported as 1.0 MΩ and 47 pF. The dependence of the percent errors, $\Delta Z'$% and $\Delta Z''$%, on the frequency in hertz is reported in Figure 6b. For the entire frequency range, error is lower than 2%, which indicates that the HCP does not affect the electric measurements in the investigated frequency range.

Using the same RC$_{||}$ test circuit, the HCP was tested over a range of temperatures (284−347 K) and CO_2 pressures (0−6 MPa). The results are reported in Figure 7. A slight decrease of the maximum peak frequency domain, f_{peak}, is observed with increasing gas pressure, while a significant increase is observed with increasing temperature. The smaller increase with f_{peak} is due to the effect of temperature on the circuit's elements. At constant temperature, the difference between f_{peak} in air and f_{peak} in CO_2 at high pressure is less than 0.5% (data not shown).

The capacitance of the RC$_{||}$ test circuit as a function of temperature and pressure is reported in Figure 8. The capacitance increases by about 4.2% with increasing temperature over the 70 K temperature range and CO_2 pressures from 0 to 6 MPa, whereas the variation in the resistance under CO_2 is very small, only 0.05%. It is clear that both resistance and capacitance increase with increasing temperature and pressure, but the values are comparable within experimental error. Taken together, the above results illustrate that the HCP cell is highly reliable for

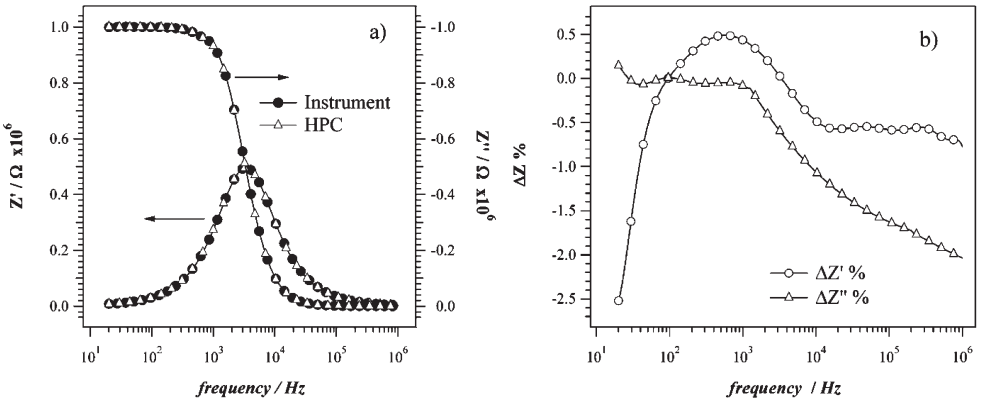

Figure 6. (a) Impedance response of RC$_{\|}$ test circuit connected directly to the instrument (●) and to the high pressure cell (Δ). Z'' and Z' represent the imaginary and the real part of the impedance, respectively. Arrows indicate the ordinate axis for the experimental data. (b) Percent error of impedance differences $\Delta Z'$ and $\Delta Z''$ measurements as a function of frequency of the RC$_{\|}$ test circuit measured embedded with the HCP cell and directly with the HP4284A Precision Analyzer. $\Delta Z'\% = (Z_{HCP}' - Z_{direct}')/(Z_{direct}') \times 100$ and $\Delta Z''\% = (Z_{HCP}'' - Z_{direct}'')/(Z_{direct}'') \times 100$ where the indices HCP and direct indicate the impedance of the test circuit measured with the HCP cell and connected directly to the HP4284A Precision Analyzer, respectively.

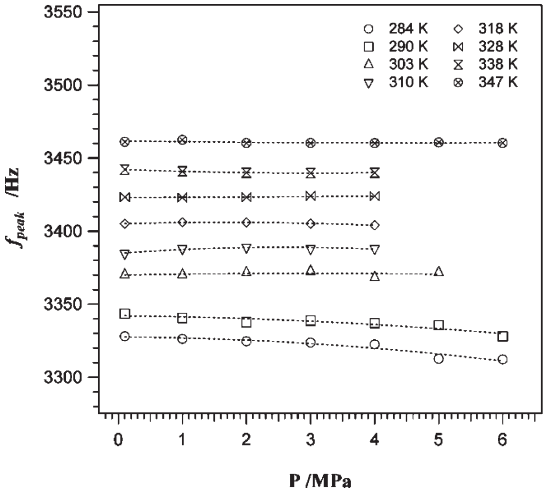

Figure 7. Peak frequency, f_{peak}, of the RC$_{\|}$ test circuit versus CO_2 pressure and temperature. The lines are a guide for the eye only.

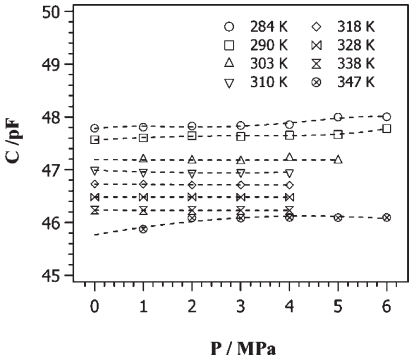

Figure 8. CO_2 pressure and temperature dependence of the capacitance, C, of the RC$_{\|}$ test circuit measured in the HCP cell. The lines are a guide for the eye only.

measuring the permittivity spectra of materials with extremely low dielectric constants, such as fluid CO_2.

Electric Measurement of CO_2. It is important to understand the electric behavior of CO_2 before using supercritical CO_2 as a low dielectric solvent. This section examines interactions in supercritical CO_2 focusing on the interaction between CO_2 molecules and CO_2 aggregates as a function of temperature and pressure. The profiles of the real component of the CO_2 permittivity, ε', as function of pressure are shown in Figure 9 over the pressure range from 0.1 to 6 MPa. It is observed that in the explored frequency range, the values of ε' are essentially independent of frequency as expected (data not shown) but are significantly dependent on pressure and temperature. At 323 K, the values of ε' increase slightly with increasing pressure, but at 287 K there is a steep increase of ε' from 1.03 to 1.6. At 287 K, the phase transition of CO_2 from a gas to a liquid can be observed at about 4.97 MPa.[21] The phase transition results in an increase in the density (ρ) of CO_2,[22] and it is well-known[23] that the permittivity of a substance increases as the number of the molecules per volume unit increases. For the system under investigation, the dependence of the permittivity on ρ follows eq 1.

$$\left(\frac{\varepsilon - 1}{\varepsilon + 2} - \frac{\varepsilon_\infty - 1}{\varepsilon_\infty + 2}\right)\frac{M}{\rho} = \frac{N}{3\varepsilon_o} \times \frac{\mu^2}{3kT} \qquad (1)$$

In this equation, ε is the permittivity, ε_∞ is the permittivity at infinite frequency, M is the molecular weight of CO_2, ρ is its density, N is Avogadro's number, ε_o is the permittivity in a vacuum, k is the Boltzmann constant, T is the temperature, and μ is its dipole moment.

The ε' values measured with the HCP are in good agreement with those measured by Michels and Michels,[24] as observed by the overlap of the ε' data shown in Figure 9.

On the basis of its structure, CO_2 is generally regarded as a nonpolar molecule, but supercritical CO_2 has proven to be miscible with a number of materials, including many that are polar.[25] The miscibility of CO_2 with polar materials would indicate that intermolecular interactions result in CO_2 aggregates that have a nonzero dipole moment. Recently a number of neutron diffraction, spectroscopy, and simulation studies have examined the structure of CO_2 at higher pressures and in condensed phases.[22,25−31] These studies

dx.doi.org/10.1021/jp2043448 |J. Phys. Chem. B 2011, 115, 9014–9021

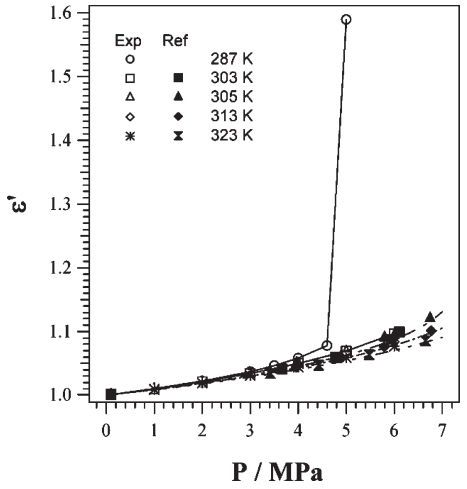

Figure 9. Measured real component of the CO_2 permittivity (ε') as function of pressure. The reference data[24] is taken from Michels and Michels.

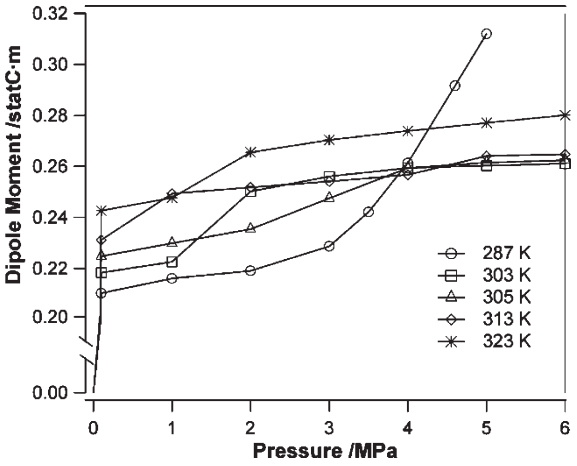

Figure 10. Dipole moment (μ) of CO_2 calculated with Debye equation[23] as a function of pressure. As pressure approaches the limit of 0 MPa, μ approaches 0 D.

have shown that a number of possible geometries for CO_2 dimers exist, such as the T-shaped and slipped parallel geometries.[27,28,30−33] The dipole moment of the slipped parallel geometry has been estimated to be very low, approximately 0.04 D,[29] but the dipole moment of the T-shaped geometry is estimated to be somewhat higher, approximately 0.30 D.[26,29] The slipped parallel geometry seems to be preferred at lower pressures in the gas state, while the T-shaped geometry becomes more dominant at the higher pressures and in the fluid phase.[27,28,31]

The permittivity ε' can be used to calculate the dipole moment of CO_2 using the Debye equation (eq 1).[23] In this equation the density is determined as described by Sievers,[34] and the value of ε_∞ is calculated as the square of the refractive index, n^2.[8] The refractive index is determined by eq 2 reported by Fehrenbacher et al.:[35]

$$\left(\frac{n^2-1}{n^2+2}\right)\frac{1}{\rho'} = A_R + B_R\rho' + C_R\rho'^2 \qquad (2)$$

where ρ' is the volumetric density and A_R, B_R, and C_R are the virial coefficients ($A_R = 6.649\ cm^3\ mol^{-1}$, $B_R = 1.9\ cm^6\ mol^{-2}$, and $C_R = -287\ cm^9\ mol^{-3}$). Thus, the CO_2 dipole moment determined with eq 1 varies between 0 and 0.3, increasing with increasing pressure as shown in Figure 10. Dipole moments in this range seem to indicate a mix of geometries, with the lower dipole geometries existing at lower pressures (0.2 D at P = 0.1 MPa). The increasing dipole moment at higher pressures supports a shift toward a T-shaped geometry of CO_2 dimers.

There is no CO_2 dielectric relaxation observed in the frequency range from 100 Hz to 1 MHz, and the imaginary component of the permittivity remains very low, $\varepsilon'' \approx 10^{-4}$, on the order of the experimental error. The results indicate that BES−HCP is a powerful and simple spectroscopic tool in the study of the structural distortion of CO_2 under high pressure and in its supercritical state.

Electric Response of PVC under CO_2 Pressure. As previously discussed, CO_2 is not a simple inert gas with respect to polymer films. As a function of pressure and temperature, it interacts with the polymers, modifying their structures. It has been demonstrated that CO_2 is soluble in many polymers and can modulate their properties, such as the glass transition and melting temperatures, viscosity of the mixture, etc.[4,36] To investigate these effects in detail by BES−HCP spectroscopy, the permittivity spectra of the PVC polymer film were measured after introducing CO_2 into the HCP. The BES−HCP spectrum of PVC−CO_2 was collected every 10 min until equilibrium was reached, as indicated by no further changes in the spectrum.

PVC is a B-type polymer, i.e., the dipole moment of its repeat units is located in the polymer backbone and perpendicular to the chain axis, with little correlation between the repeat unit dipole moment of different chains.[8,37] PVC is strongly polar due to the carbon−chlorine bonds,[38−40] exhibits both α and β relaxation processes and has a dielectric constant that increases to approximately 12 at high temperatures. The interactions within PVC and between PVC and CO_2 are weak. Therefore, PVC is a good material for a preliminary study using the BES−HCP setup because it avoids any complications arising from intermolecular reactions of starting components.

In Figure 11, the real (ε') and imaginary (ε'') components of the permittivity of the PVC−CO_2 system are reported as a function of frequency and CO_2 pressure. For clarity, only four pressure values are reported. For ε' and ε'' the spectra at atmospheric pressure are very different from those measured at higher pressures. As expected, the ε' and ε'' profiles shift toward higher frequencies with increasing pressure, thus indicating that plasticization of PVC is occurring by CO_2 absorption. ε'' shows clearly that the α-relaxation peak typical of PVC shifts toward higher frequency values. This trend indicates unequivocally that the dissolution of CO_2 within the bulk polymer film reduces the polymer interchain interactions and increases the chain mobility. These results are in agreement with the decrease of the PVC glass transition temperature with CO_2 pressure previously reported,[41] where it was stated that the T_g of PVC decreases in the order 348.15 > 320 > 310.2 K at pressures of 0.1 > 2.0 > 4.0 MPa, respectively.

To examine the relaxation phenomena of the PVC−CO_2 system in detail, ε' and ε'' were fitted simultaneously using the

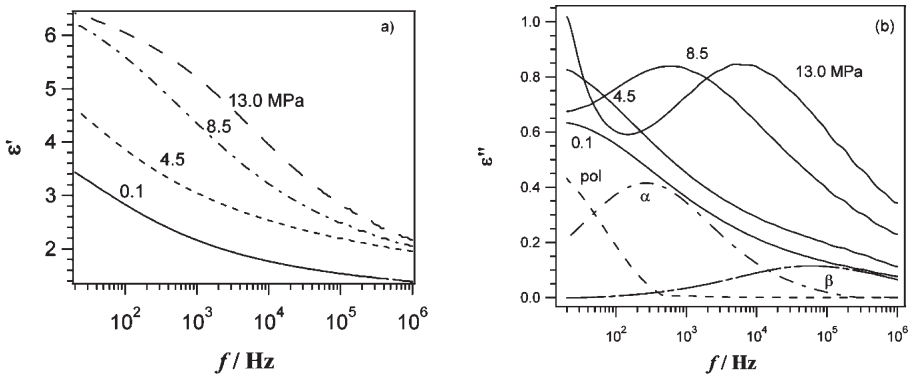

Figure 11. Real (a) and imaginary (b) components of the permittivity, ε, of the PVC film as function of frequency and CO_2 pressure. The spectra were recorded at 343 K. The fitted α and β relaxation peaks and the electrode polarization (pol) are determined by eq 3.

generalized Havriliak−Negami equation:[8,42]

$$\varepsilon^*(\omega) = \varepsilon' - i\varepsilon'' = \varepsilon_\infty - i\left(\frac{\sigma_0}{\varepsilon_0\omega}\right)^s + \sum_{k=1}^{n}\frac{\Delta\varepsilon_k}{(1 + (i\omega\tau_k)^{\alpha_k})^{\beta_k}} \quad (3)$$

where τ_k is a characteristic relaxation time related to the peak frequency f_k ($\tau_k = (2\pi f_k)^{-1}$), σ_0 is the direct current conductivity, s is a parameter that defines the frequency dependence of the conductivity term, $\Delta\varepsilon_k$ is the relaxation strength of the kth relaxation event, α_k and β_k are shape parameters which account for the symmetric and asymmetric broadening of kth relaxation peak. The spectra of the PVC−CO_2 system are fitted assuming two relaxations. The lower frequency peak is assigned as an α-relaxation process associated with the segmental motion of the polymer, while the higher one is correlated to a β-process which is attributed to the relaxation of local dipoles of the PVC chain repeat units. The width of the β-relaxation peak is similar to that of the α-relaxation at low pressures. In addition, the width of the β-relaxation peak is dependent on pressure, while that of the α-relaxation peak is not. The independence of the width of the α-relaxation peak on pressure suggests that the segmental motion is not affected by interchain interactions. The β-relaxation as expected is strongly dependent on the concentration of CO_2 in the bulk material.

The dependence of the frequency peak maximum on CO_2 pressure for both relaxation processes are shown in Figure 12. Both relaxation processes show parallel behavior, an initial decrease at pressures less than 5 MPa, followed by an increase at higher pressures. This behavior suggests competing effects of hydrostatic pressure and plasticization phenomena of CO_2. Specifically, (a) at $P < 5$ MPa, the effect of hydrostatic pressure is predominant and thus the α and β dynamics of the polymer chains are reduced as the pressure increases, and (b) at $P > 5$ MPa, the plasticization effect of CO_2 is predominant. The α and β dynamics become faster as CO_2 pressure increases, shifting the maximum of the ε'' relaxation peaks toward higher frequencies. These results are confirmed by the dependence of the dielectric strength of the α and β peaks on pressure shown in Figure 13. The dielectric strength of the α-relaxation is higher than that of the β-relaxation under CO_2 pressure, a trend which is supported by the literature.[8] The α-relaxation process exhibits an increase in the dielectric strength at approximately 5 MPa, while the β-relaxation shows a decrease at approximately 10 MPa. The trend in the dielectric strength of the α-relaxation

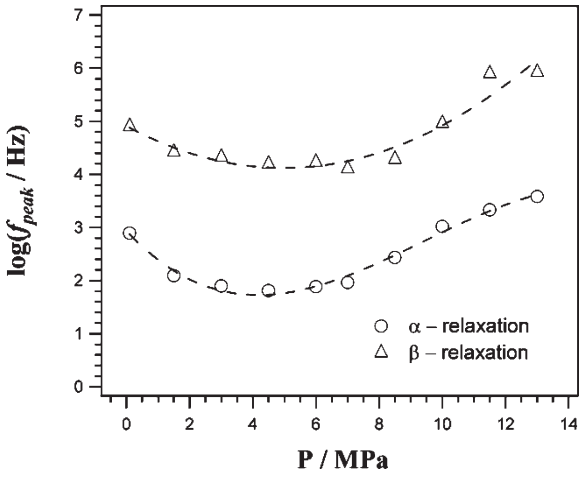

Figure 12. Peak frequency, f_{peak}, as function of the experimental CO_2 pressure for the PVC−CO_2 system. The frequency values $f_{max} = \omega_p/2\pi$ are determined from the relationship $\omega_p = 1/\{\tau_k[\sin(\alpha_k\pi/(2+2\beta_k))]^{1/\alpha_k} \cdot [\sin(\alpha_k\beta_k\pi/(2+2\beta_k))]^{-1/\alpha_k}\}$,[8,37] which takes into consideration the relaxation times determined from the Havriliak−Negami equation and the shape parameters of the peaks. The α-relaxation is associated with the segmental motion of the polymer. The β-relaxation is associated the relaxation of local dipoles of the PVC chain repeat units.

process ($\Delta\varepsilon_\alpha$) confirms that the plasticization effect of the PVC resulting from the dissolution of the gas into the polymer takes place predominantly at pressures greater than 5 MPa. Under these pressure conditions, as the gas dissolves into the polymer, the interactions between polymer chains are reduced, allowing increased chain mobility. The enhanced chain mobility also is revealed by the increase in the frequency of the α-peak with increased pressure. At 13 MPa and 343 K, the frequency of the peak is 3600 Hz, which corresponds to a temperature higher than 373 K at ambient pressure. Higher chain mobility means that the chain can respond more easily to the electric field, resulting in the increased dielectric strength of the α-relaxation process. The trend in the β-relaxation is the result of an increased interaction of the PVC repeat unit dipole with the small dipole of the CO_2 aggregates at high pressures, greater than 8 MPa, which results in an ordering of the local dipoles and the consequent decrease in the dielectric strength. In summary, the results described in this section

dx.doi.org/10.1021/jp2043448 |J. Phys. Chem. B 2011, 115, 9014–9021

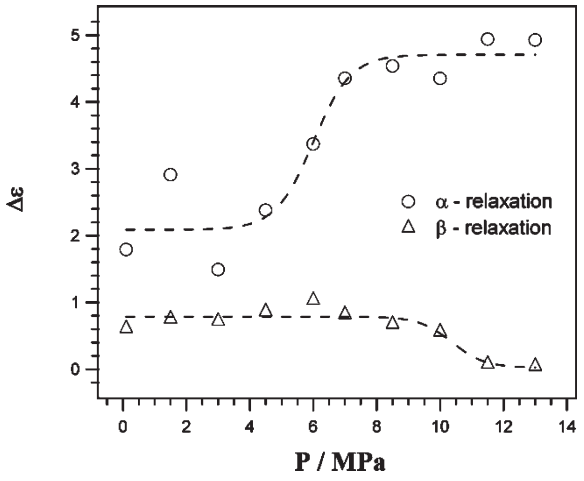

Figure 13. Dielectric strength of the α-relaxation and β-relaxation phenomena of the PVC film under CO_2 pressure at 343 K. The lines are a guide for the eyes only. The α-relaxation is associated with the segmental motion of the polymer. The β-relaxation is associated with the relaxation of local dipoles of the PVC chain repeat units.

prove that BES−HCP is of crucial importance in the characterization of the polymer−CO_2 interactions.

CONCLUSIONS

A high CO_2 pressure cell, which can operate up to 15 MPa and 353 K, was designed and constructed for electric measurements of bulk materials. The BES−HCP system can measure the electric spectra of low dielectric constant materials under CO_2 pressure without electrical dispersion or gas leakage. Using this cell, the electric response of gas and liquid CO_2 was measured up to 6 MPa in the temperature range from 287 to 323 K. The dipole moment of CO_2 increased with increasing temperature, which most likely corresponds to an increased fraction of molecules in T-shaped dimers. This result shows that the HCP cell can be useful to study intermolecular interactions in high pressure and supercritical CO_2. No relaxation peaks were present in the dielectric profile of CO_2, thus making it simpler to measure the PVC−CO_2 system. Analysis of the PVC−CO_2 spectra revealed the complex behavior of this system. The presence of high pressure CO_2 can result in two contrary phenomena: (1) the effect of increased hydrostatic pressure, which reduces the free volume and therefore the segmental motion within PVC; (2) plasticization of the polymer by supercritical CO_2 that leads to a reduction in the glass transition temperature due to increased mobility of the polymer chains. The dominant phenomenon depends on the concentration of CO_2 dissolved inside the polymer which is a function of both temperature and pressure. An increase in the maximum peak frequency of the relaxation phenomena occurs at higher pressures, indicating that the plasticization effect is not significant until the CO_2 pressure is sufficiently high. In addition, the decrease in the dielectric strength of the β-relaxation mode provides evidence of the interaction of the slightly polar CO_2 aggregates and the local dipoles of the PVC chain repeat units. Therefore, BES−HCP measurements have shown to be extremely important in the characterization of polymer−CO_2 interactions.

An additional conclusion refers to the possibility of using CO_2 as a solvent. CO_2 is an extremely attractive solvent for electric measurements because its dielectric constant is very low, close to 1. Additionally, despite a near-zero dipole moment, it has the ability to solvate many materials.

APPENDIX A: BES−HCP SIZE

The geometric parameters of the HCP are summarized in Table 1. These metric parameters have been selected considering the dimensions of the measuring system, sample support, and stainless steel commercial cylinder and the ability to support the extreme experimental conditions (temperatures up to 353 K and pressures up to 13 MPa). The wall thickness of the 4.5 mm was designed based on the Von Mises criterion,[43]

$$\frac{\sqrt{3}K^2 P_{max}}{K^2 - 1} \leq \sigma_{adm} \qquad (A.1)$$

where P_{max} is the highest applicable pressure [13 kg_f/mm^2], σ_{adm} is the highest admissible stress in the material and K is the diameter ratio d_e/d_i, where d_i and d_e are equal to the vessel internal and external diameters, respectively. In this case, σ_{adm} (= $\sigma_{s,T}/f_s$) is equal to 10.56 kg_f/mm^2 considering a safety coefficient (f_s) equal to 1.5. The value of the material stress ($\sigma_{s,T}$), as function of the temperature is determined by:[43]

$$\sigma_{s,T} = \sigma_{s,20°C}[1 - 0.0015(T - 20)] \qquad (A.2)$$

where T is the operative temperature in degrees Celsius, which is assumed to be equal to 373 K. The value of $\sigma_{s,20\,°C}$ is 18 kg_f/mm^2 which corresponds to the yield strength of stainless steel AISI 316. An internal diameter of 64 mm was chosen as a compromise between the maximum dimension of the sample and the minimum volume of the cell.

AUTHOR INFORMATION

Corresponding Author
*E-mail: vito.dinoto@unipd.it.

ACKNOWLEDGMENT

The authors thank Mr. C. Bedin and Eng. M. Petterle for their assistance in construction of the cell and data collection. This work was financed by Italian MURST project PRIN2008, entitled "Direct polymer electrolyte membrane fuel cells: synthesis and study in prototype cells of hybrid inorganic−organic membranes and electrode materials".

REFERENCES

(1) Wissinger, R. G.; Paulaitis, M. E. *J. Polym. Sci., Part B: Polym. Phys.* **1987**, *25*, 2497.
(2) Striolo, A.; Favaro, A.; Elvassore, N.; Bertucco, A.; Di Noto, V. *J. Supercrit. Fluids* **2003**, *27*, 283.
(3) Tominaga, Y.; Kwak, G. H.; Hirahara, S.; Asai, S.; Sumita, M. *Polymer* **2003**, *44*, 4769.
(4) Tomasko, D. L.; Li, H.; Liu, D.; Han, X.; Wingert, M. J.; Lee, L. J.; Koelling, K. W. *Ind. Eng. Chem. Res.* **2003**, *42*, 6431.
(5) Vezzù, K.; Betto, V.; Elvassore, N. *Biochem. Eng. J.* **2008**, *40*, 241.
(6) Di Noto, V.; Vezzù, K.; Pace, G.; Vittadello, M.; Bertucco, A. *Electrochim. Acta* **2005**, *50*, 3904.
(7) Vezzù, K.; Zago, V.; Vittadello, M.; Bertucco, A.; Di Noto, V. *Electrochim. Acta* **2006**, *51*, 1592.
(8) *Dielectric Spectroscopy of Polymeric Materials: Fundamentals and Applications*; Runt, J. P.; Fitzgerald, J. J., Eds.; American Chemical Society: Washington, DC, 1997.

(9) Hourri, A.; St-Arnaud, J. M.; Bose, T. K. *Rev. Sci. Instrum.* **1998**, *69*, 2732.
(10) Piazza, S.; Galia, A.; V., I.; Filardo, G. Investigation of Solute Behaviour in Supercritical Fluids by Dielectric Spectroscopy. Presented In *6th International Symposium on Supercritical Fluids*; ISASF: Nancy Cedex, France, 2003.
(11) Galia, A.; Scialdone, O.; Begue, G.; Piazza, S.; Filardo, G. *J. Supercrit. Fluids* **2007**, *40*, 183.
(12) Goldfarb, D. L.; Fernandez, D. P.; Corti, H. R. *Fluid Phase Equilib.* **1999**, *158*−*160*, 1011.
(13) Hirota, S.-I.; Tominaga, Y.; Asai, S.; Sumita, M. *J. Polym. Sci., Part B: Polym. Phys.* **2005**, *43*, 2951.
(14) Matsumiya, Y.; Inoue, T.; Iwashige, T.; Watanabe, H. *Macromolecules* **2009**, *42*, 4712.
(15) Matsumiya, Y.; Inoue, T.; Watanabe, H.; Kihara, S.; Ohshima, M. *Nihon Reoroji Gakkaishi* **2007**, *35*, 155.
(16) Ibbs, T. L.; Wakeman, A. C. R. *Proc. R. Soc. London, Ser. A* **1932**, *134*, 613.
(17) Keyes, F. G.; Kirkwood, J. G. *Phys. Rev.* **1930**, *36*, 754.
(18) Zahn, C. T. *Phys. Rev.* **1926**, *27*, 455.
(19) McCrum, N. G.; Read, B. E.; Williams, G. *Anelastic and dielectric effects in polymeric solids*; Dover Publications: New York, 1967.
(20) Di Noto, V.; Vittadello, M.; Zago, V.; Pace, G.; Vidali, M. *Electrochim. Acta* **2006**, *51*, 1602.
(21) Perry, R. H.; Green, D. W.; Maloney, J. O. *Perry's Chemical Engineers' Handbook*, 7th ed.; McGraw-Hill: New York, 1997.
(22) Ishii, R.; Okazaki, S.; Odawara, O.; Okada, I.; Misawa, M.; Fukunaga, T. *Fluid Phase Equilib.* **1995**, *104*, 291.
(23) Ku, C. C.; Liepins, R. *Electrical properties of polymers: Chemical principles*; Hanser: Munich, 1987.
(24) Michels, A.; Michels, C. *Philos. Trans. R. Soc. Lond. Ser. A:* **1933**, *231*, 409.
(25) Raveendran, P.; Ikushima, Y.; Wallen, S. L. *Acc. Chem. Res.* **2005**, *38*, 478.
(26) Barton, A. E.; Chablo, A.; Howard, B. J. *Chem. Phys. Lett.* **1979**, *60*, 414.
(27) Cipriani, P.; Nardone, M.; Ricci, F. P.; Ricci, M. A. *Mol. Phys.* **2001**, *99*, 301.
(28) Ishii, R.; Okazaki, S.; Okada, I.; Furusaka, M.; Watanabe, N.; Misawa, M.; Fukunaga, T. *J. Chem. Phys.* **1996**, *105*, 7011.
(29) Jucks, K. W.; Huang, Z. S.; Dayton, D.; Miller, R. E.; Lafferty, W. J. *J. Chem. Phys.* **1987**, *86*, 4341.
(30) Saharay, M.; Balasubramanian, S. *J. Chem. Phys.* **2004**, *120*, 9694.
(31) Saharay, M.; Balasubramanian, S. *J. Phys. Chem. B* **2007**, *111*, 387.
(32) Tsuzuki, S.; Tanabe, K. *Comput. Mater. Sci.* **1999**, *14*, 220.
(33) Zhang, Y.; Yang, J.; Yu, Y.-X. *J. Phys. Chem. B* **2005**, *109*, 13375.
(34) Sievers, U. *Die thermodynamischen Eigenschaften von Kohlendioxid*, 1st ed.; VDI-Verlag: Düsseldorf, 1984.
(35) Fehrenbacher, U.; Jakob, T.; Berger, T.; Knoll, W.; Ballauff, M. *Fluid Phase Equilib.* **2002**, *200*, 147.
(36) Vezzù, K.; Bertucco, A.; Lucien, F. P. *AIChE J.* **2008**, *54*, 2487.
(37) *Broadband Dielectric Spectroscopy*; Schonhals, A.; Kremer, F., Eds.; Springer: Berlin, 2003.
(38) Naoki, M. *J. Chem. Phys.* **1989**, *91*, 5030.
(39) Reddish, W. *J. Polym. Sci., Polym. Symp.* **1966**, *No. 14*, 123.
(40) Utracki, L. A.; Jukes, J. A. *J. Vinyl Technol.* **1984**, *6*, 85.
(41) Zhang, Z.; Handa, Y. P. *J. Polym. Sci., Part B: Polym. Phys.* **1998**, *36*, 977.
(42) Vittadello, M.; Suarez, S.; Chung, S. H.; Fujimoto, K.; Di Noto, V.; Greenbaum, S. G.; Furukawa, T. *Electrochim. Acta* **2003**, *48*, 2227.
(43) Manning, W. R. D.; Labrow, S. *High Pressure Engineering*; Leonard Hill: London, 1971.